THERMAL DIFFUSIVITY MEASUREMENT OF POROUS SILICON LAYER (P-TYPE) USING PHOTO-ACOUSTIC TECHNIQUE

[1]MOHAMMED JABBAR HUSSEIN, [2]W. MAHMOOD MAT YUNUS, [3]HALIMAH MOHAMED KAMARI, [4]AZMI ZAKARIA

[1,2,3,4]Department of Physics, Faculty of Science, Universiti Putra Malaysia, 43400 UPM Serdang, Malaysia. [1]Laser & Electro-Optic Centre, Directorate of Material Research, Ministry of Science & Technology, Iraq
Email: [1]mohammed55865@yahoo.com

Abstract-Thermal diffusivity for porous silicon p-type was measured using the photoacoustic technique. The porous silicon samples were prepared under the current densities of 10 to 30 mA/cm^2 whilst the etching time ranged from 20 to 80 min. The thermal diffusivity of the porous silicon was obtained by graph fitting. Findings from measurement showed that the thermal diffusivity decreased with increasing etching time and current densities.

Keywords-Etching Time, Thermal Diffusivity, Current Densities, Porous Silicon, Photoacoustic

I. INTRODUCATION.

Photoacoustic (PA) and photothermal (PT) techniques have been established as diagnostic methods with sensitivity to the dynamics of photo-excited carriers. This technique has important advantages due to its great versatility as the sensitive, non-invasive and non-destructive character for the evaluation of material parameters, as well as in the semiconductor industry for characterizing processes in the manufacturing of microelectronic devices. Since the generation of excess carriers will produce thermal waves due to the carrier thermalization and recombination processes, the carrier transport properties of semiconductor materials can be quantified from PA phase signal experimental data [1–6]. The underlying principles of the PA effect have been studied for more than a century. It is termed as PA because the indirect acoustic method in detection of the PT eating. Alexander Graham Bell had discovered the early concept of the PA effect when he tried to explain the operation of his photo-phone. Through various experiments on PA effect on solids, he discovered that when a periodically interrupted beam of sunlight shines on a solid in an enclosed cell, an audible sound could be heard by means of hearing tube attached to the cell. Bell's discovery was regarded as a part of the family of PT phenomena encompassing many effect produced by the heat generated in a sample due to the absorption of electromagnetic energy. Tyndah and Withem Roentgen (1997) confirmed Bells experiment on gases. They found that an acoustic signal could also be produced when the gas in an enclosed cell is illuminated with modulated light. Progress in the PA field was
hindered due to the limitation of hearing tubes used as detectors in the early experiment. After fifty years of none adventure for the PA technique, the use of microphone now became the new detector. The theory of the PA effect in solid sample was first described by Rosencwaig and Gersho [3, 7]. Two different regimes hold for this theory that, the thermally thin and the thermally thick sample regimes. For a thermally thin regime, the amplitude of PA signal decreases as . The microphone as a new detector was used to re-investigate the PA effect with gases. In this method, the gas in the PA cell absorbs and converts photons into kinetic energy (heat) of the gas molecules, thus giving rise to pressure fluctuations within the cell. The sample thermal diffusivity (TD), α_s can be obtained from the signal amplitude data as a function of modulation frequency by fitting the data to the equation [7]. All the data acquisition was microcomputer controlled. The TD is obtained from the modulation frequency dependence of the detected PA signal, as discussed in detail in Refs [9,11,12]. That is, using the thermal diffusion model for the PA effect, the measurement signal *S* in the modulation frequency range for the for the case of thermally thick regime may be written as [8,11]

$$S = \left(\frac{A}{f}\right) exp(-b\sqrt{f}) \qquad (1)$$

where,

$$\alpha_s = \pi \left(\frac{l_s}{b}\right)^2 \qquad (2)$$

Here A and b are constants, and l_s is the sample thickness. The TD is obtained by fitting experimental data with equation (1). From it b can be obtained and thus TD can be evaluated from equation (2).

The porosity is defined as a fraction of void within the porous silicon (PSi) layer and can be easily obtaining by weight measurements. The wafer is weight before porous m_1, just after porous m_2 , and after rapid dissolution of the porous layer PSi in a 3% KOH solution m_3. The porosity is given by the following equation

$$P(\%) = \frac{m_1 - m_2}{m_1 - m_3} \quad \ldots\ldots\ldots \qquad (3)$$

Thickness porous as given by .

$$d = \frac{m_1 - m_2}{\rho s} \ldots\ldots\ldots\ldots\ldots\ldots\ldots\ldots\ldots\ldots (4)$$

where the and s the Si density and the etched surface area, also The thickness of the porous was measured by a profilometer (Ambios Technology XP-200). The porous silicon (PSi) formation was obtained by electrochemical dissolution of silicon (Si) wafer in aqueous or ethanoic (HF acid) solution. In the 1970 and 1980 the interest on the porous PSi increased due to the high surface area of PSi and was found to be useful as a model of a crystalline Si surface in the spectroscopic studies [14,15], as a precursor to generate thick oxide layers on the Si, and as a dielectric layer in capacitance – based the chemical sensors [16]. Liegh Canham in 1990 published his results on red - luminescence. From the PSi that was explained in terms of quantum confinement of carriers in nano-crystals of Si which are present in the pore walls, since that time, the interest of researchers and technologists to this material (and other porous semiconductors as well) is constantly growing and the number of publications dedicated to this type of materials increase by year. Finding the efficient visible light emission from the PSi caused by an increased number of works focused on creating Si-based opto-electronic switches, displays, and lasers. During the last decade, researches on the optical properties of PSi have become very intense. In present work the TD measurement by PA technique on the PSi prepared by electrochemical method under different current density and varying etching time will be presented.

II. PREPARATION POROUS SILICON

All PSi samples were prepared on (100) n-type Si single crystal wafers of 537 μm thickness. The wafers were cleaned into approximately 2 cm square substrates. Prior to preparation, the Si substrates were cleaned by sonification for 5 min in ethanol, and acetone. A Si substrate was placed at the bottom of a cylindrical Teflon cell and fixed by an aluminium plate as a backing material. A platinum rod serves as a cathode perpendicular to the Si surface at a distance of (1 cm). The current density and etching time were applied at solution of hydrofluoric (HF) acid and ethanol (purity 99.90%) in the volume ratio of 1:1. The HF acid is an essential ingredient for the anodal etching of Si. Ethanol is an electrolyte to enhance the homogeneity and uniformity of the PSi surface because it acts as a promoting agent to increase the wettability of PSi surface and to remove the extraneous H_2 bubbles that appear during the anodic etching process. In fact, ethanol solutions infiltrate the pores, while purely aqueous HF solution do not[13]. This is very important for the lateral homogeneity and the uniformity in depth of the PSi layer. A digital DC current source (ADCMT6243) was used to supply constant current. Fig. 1 shows the schematic diagram of all the elements used for the preparation of PSi. To generate the electron hole pairs, the surface of sample was illuminated with 300 W halogen lamp (Osram, ELH93518) during anodisation. For all samples, a voltage of 50 V was applied to the halogen lamp for illumination. Three set of samples were prepared at current densities of 10, 20, and 30 mA/cm^2, and all sets were etched with etching time of 20, 40, 60, and 80 min. Fig. 2 shows the PSi samples prepared by electrochemical method. This method used to determine semiconductor energy gap[21.22].

The samples prepared with current density of 20 mA/cm^2 and etching time 40 min. The NaOH used to remove the PSi to measured porosity[10].

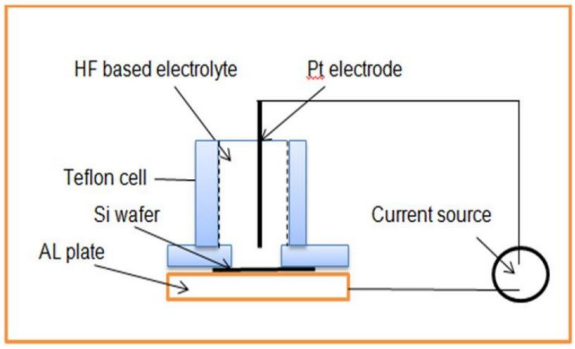

Figure 1: Schematic of electrochemical etching cell for anodisation of (PSi) samples

III. EXPERIMENTAL SET UP

PA methods are successfully applied to determine the values of thermophysical parameters of PSi [18, 19]. The experimental set up used for the present study is schematically shown in Fig. 2. The set-up consists of a He-Ne laser beam, an open PA cell and a PT detection system. The laser beam after being mechanically chopped by an optical chopper was focused onto a sample kept inside the PA cell. As a result of the periodic heating, the heat generated in the sample is transferred to the gas in contact. Hence, the air in the chamber oscillates at the chopping frequency, causing diaphragm deflection, which generates a voltage across the load resistor. The generated PA signal was than amplified by a pre-amplifier and analyzed using a lock-in amplifier before collecting data by Lab View software. All measurements were carried out under room temperature.

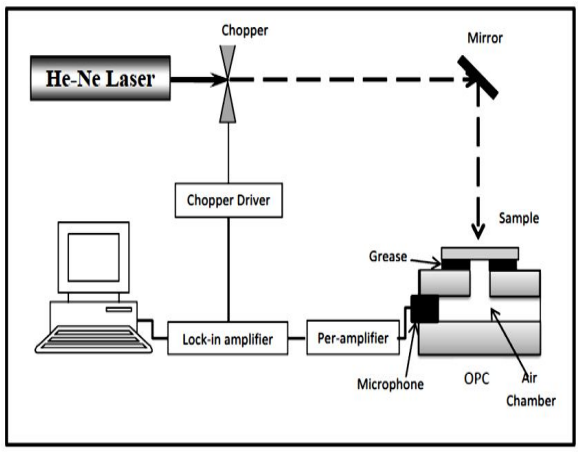

Figure 2: Experimental set up of open acoustic cell detection technique

IV. RESULTS

The results for the TD measurement are shown in Fig. 3 for the PSi sample prepared under etching time of 40 min and of current density 20 mA/cm^2. The TD of the sample was calculated using equation (2). For the sample (J = 20 mA/cm^2/s and t = 40 min) conditions, the calculated TD
(α) was (0.246±0.006) cm^2/s. Shown in Fig. 3 is the PA signal against frequency. Observation also showed that for the (J=20 mA/cm^2 and t=60 min) conditions, the PA signal significantly dropped with increase in frequency whilst the fitting analysis showed very good agreement with equation 1. The calculated α from fitting was (0.237±0.008) cm^2/s. While for pure Si, the value obtained by the similar technique was 0.237±0.008 cm^2/s and it is within 0.84 – 0.97 cm^2/s as obtained by Alvarado and Vargas[9].

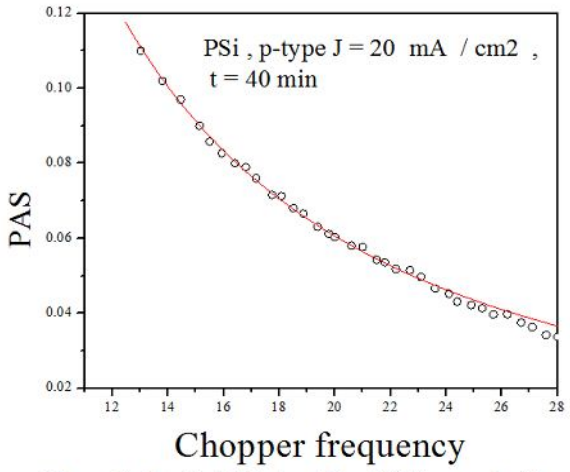

Figure 3: Typical PA signal for (PSi) sample (J = 20 mA/cm^2 and t = 40 min)

For all the measurement carried out, a summary for all the results including the current density, thickness porous, α, and etching time are presented in Table 1.

Table 1: Summary of TD, current density, etching time, and porosity of Psi

Current density mA/cm^2	Etching time min	Thickness porosity μm	Thermal diffusivity cm^2/s	Porosity
10	20 min	4	0.277	20.33
	40 min	9.4	0.257	40.6
	60 min	19.9	0.243	48.2
	80 min	30.8	0.238	56.2
20	20 min	16.8	0.258	29.04
	40 min	22.2	0.246	50.3
	60 min	35.9	0.237	57.6
	80 min	45.0	0.236	65.8
30	20 min	27.4	0.235	38.2
	40 min	33.2	0.232	59.6
	60 min	43.8	0.228	68.7
	80 min	58.8	0.224	78.2

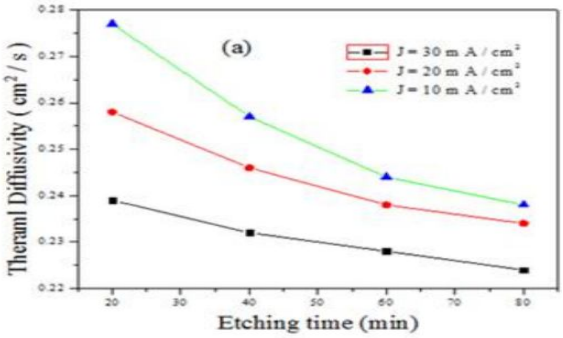

Figure 4: Variations of the TD as function of etching time for different current densities

Based on the results presented in Table 1, both the etching time and current densities were plotted against the TD obtained on separate graphs as shown in Fig.'s 5 and 6 respectively. Fig. 4 show the TD decreased quickly in etching time 40 min also the TD decreased with etching time increasing. Careful observation on Fig. 5 shows that as current density increases, the TD values also decreases. The decrease in TD for the 10 mA current density experienced a sharp drop from 20 to 60 min. This drop might be due to the small amount of current passing through the sample which takes longer time to either vibrate or expand as the case may be. However, the decrease in TD for all samples is sequentially obtained at each etching time. This behaviour can also be attributed to good sample preparation technique. The average TD obtained for the different 10, 20, and 30 mA/cm^2 current densities are 0.253, 0.244, and 0.231 cm^2/s, respectively. Fig. 4 shows the decrease of TD with increase in etching time as observed by Kasra et al [20]. This decrement of TD is caused by the reduction of mean free path due to phonon confinement in the porous structure and to the scattering at boundaries of the inner surface of the PSi [18]. The least TD was measured for the 80 min etching time with an average TD value of 0.232 cm^2/s, whilst the highest TD value was measured for the 20 min etching time with an average value of 0.259 cm^2/s. Shown in Fig. 6 are the SEM images for PSi samples prepared under different current density. Careful observation showed that porous of the samples increased with increasing current density which is in agreement with the result obtained for the TD values.

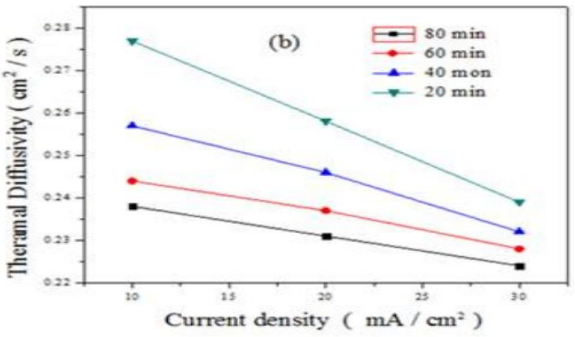

Figure 5: Variations of the TD as function of current densities for different etching time

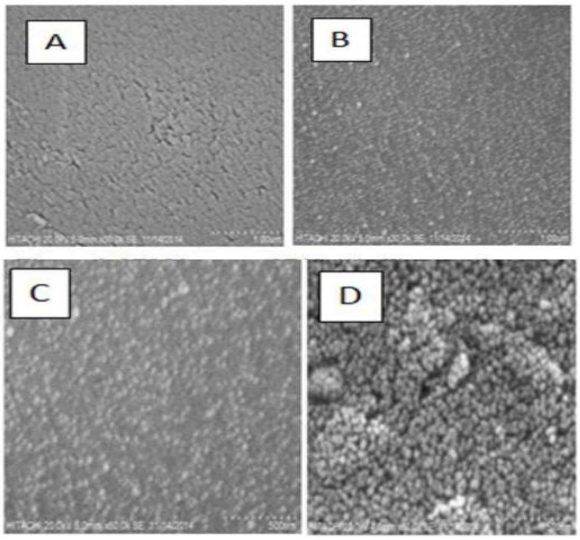

Figure 6: SEM images of PSi (A) Si wafer as scale 1µm (B) PSi, J = 10 mA/cm^2 as scale 100 µm, t = 40 min (C) PSi J = 20 mA/cm^2 as scale 500 nm, t = 40 min (D) PSi J = 30 mA/cm^2, t = 40 min as scale 500 nm.

V. SUMMARY

Prepared PSi (p-type) was investigated to find the effect of current density and etching time on its TD using the PA technique. Findings showed that both the current density and etching time play a major role in the behaviour of the diffusivity. It is thus concluded in this study that increase in both current density and etching time decreases the TD of PSi (p-type) when measured using PA technique.

ACKNOWLEDGMENT

The authors would like to thank Physics Department in the University Putra Malaysia for providing the research facilities.

REFERENCES

[1]. Ghosh, P. K., Jana, S., Maity, U. N., & Chattopadhyay, K. K. (2006). Effect of particle size and inter-electrode distance on the field-emission properties of nanocrystalline CdS thin films grown in a polymer matrix by chemical bath deposition. Physica E: Low-dimensional Systems and Nanostructures, 35(1), 178-182.

[2]. Bisi, O., Ossicini, S., & Pavesi, L. (2000). Porous silicon: a quantum sponge structure for silicon based optoelectronics. Surface Science Reports, 38(1), 1-126.

[3]. Rosencwaig, A. (1980). Photoacoustics and photoacoustic spectroscopy. Wiley.

[4]. Mansanares, A. M., Vargas, H., Galembeck, F., Buijs, J., & Bicanic, D. (1991). Photoacoustic characterization of a two- layer system. Journal of Applied Physics, 70(11), 7046-7050.

[5]. Sheng, C. K., Mahmood Mat Yunus, W., Yunus, W. M. M., Abidin Talib, Z., & Kassim, A. (2008). Characterization of thermal, optical and carrier transport properties of porous silicon using the photoacoustic technique. Physica B:

[6]. Condensed Matter, 403(17), 2634-2638.

[7]. PRESSÕES, E. D. E. D. A. (2010). *Departamento de Engenharia Mecânica Pós-Graduação em Ciência e Engenharia de Materiais* Doctoral dissertation, Universidade Federal de Santa Catarina).

[8]. Rosencwaig, A., & Gersho, A. (1976). Theory of the Photoacoustic Effect. J. Appl. Phys, 47, 64.

[9]. Souza, S. M., Trichês, D. M., Poffo, C. M., De Lima, J. C., Grandi, T. A., & De Biasi, R. S. (2011). Structural, thermal, optical, and photoacoustic study of nanocrystalline Bi2Te3 produced by mechanical alloying. Journal of Applied Physics, 109(1), 013512-013512.

[10]. J.B. Alvarado, M.L. Vargas, Anal. Sci. 17 (2001) 309

[11]. Lai, C., Li, X., Liu, C., Guo, X., Xiang, Z., Xie, B., & Zou, L. (2014). Improvement in gravimetric measurement for determining the porosity and thickness of porous silicon using an optimized solution. Materials Science in Semiconductor Processing, 26, 501-505.

[12]. Demirel, Y. (2013). Thermodynamic analysis. Arabian Journal for Science and Engineering, 38(2), 221-249.

[13]. C.A.S. Lima, M.B.S. Lima, L.C.M. Miranda, J. Baeza, J. Freer,N. Reyes, J. Ruiz, M.D. Silva, Meas. Sci. Technol. 11 (2000) 504.

[14]. El-Brolossy, T. A. (2012). Photoacoustic measurements of optical energy gap of porous silicon as a two layer opaque material. Indian Journal of Physics, 86(1), 39-44.

[15]. Dillon, A. C., Robinson, M. B., Han, M. Y., & George, S. M. (1992). Diethylsilane decomposition on silicon surfaces studied using transmission FTIR spectroscopy. Journal of the Electrochemical Society, 139(2), 537-543.

[16]. Anderson, R. C., Muller, R. S., & Tobias, C. W. (1991). Investigations of the electrical properties of porous silicon. Journal of the Electrochemical Society, 138(11), 3406-3411.(2011). Photoacoustic study of nanocrystalline silicon produced by mechanical grinding. Physica B: Condensed Matter, 406(8), 1627-1632.

[17]. Gupta, P., Dillon, A. C., Bracker, A. S., & George, S. M. (1991). FTIR studies of H< sub> 2</sub> O and D< sub>2</sub> O decomposition on porous silicon surfaces. Surface Science, 245(3), 360-372.E. Marı´n, J. L. Pichardo, A. Cruz-Orea, P. Dı´az, G. Torres-Delgado, I. Delgadillo, J. J. Alvarado-Gil, J. G. Mendoza-Alvarez, and H. Vargas, J. Phys. D 29, 981 (1996).

[18]. Shen Q and Toyoda T 2003 Review of Scientific Instruments 74 601

[19]. Obraztsov A, Karavanskii V, Okushiy H and Watanabe H 1997,

[20]. Kasra Behzad,Wan Mahmood Mat Yunus, Zainal Abidin Talib, Azmi Zakaria, Afarin Bahrami, and Esmaeil Shahriari." Investigations of the electrical properties of porous silicon. Journal of the Electrochemical Society, 138(11), 3406-3411.(2011). Photoacoustic study of nanocrystalline silicon produced by mechanical grinding. Physica B: Condensed Matter, 406(8), 1627-1632

[21]. Sarmah, S., & Kumar, A. (2010). Optical properties of SnO_2 nanoparticles. Indian Journal of Physics, 84(9), 1211-1221.

[22]. Diana, T., Devi, K. N., & Sarma, H. N. (2010). On the optical properties of SnO2 thin films prepared by sol-gel method. Indian Journal of Physics, 84(6), 687-691.

★★★